

# Contact-Dependent Killing by Cytotoxic T Lymphocytes Is Insufficient for EL4 Tumor Regression *In Vivo*

Richard J. Beck, Maarten Slagter, and Joost B. Beltman



## Abstract

Immunotherapies are an emerging strategy for treatment of solid tumors. Improved understanding of the mechanisms employed by cytotoxic T lymphocytes (CTL) to control tumors will aid in the development of immunotherapies. CTLs can directly kill tumor cells in a contact-dependent manner or may exert indirect effects on tumor cells via secretion of cytokines. Here, we aim to quantify the importance of these mechanisms in murine thymoma EL4/EG7 cells. We developed an agent-based model (ABM) and an ordinary differential equation model of tumor regression after adoptive transfer of a population of CTLs. Models were parameterized based on *in vivo* measurements of CTL infiltration and killing rates applied to EL4/EG7 tumors and OTI T cells. We quantified whether infiltrating CTLs are capable of controlling tumors through only direct, contact-

dependent killing. Both models agreed that the low measured killing rate of CTLs *in vivo* was insufficient to cause tumor regression. In our ABM, we also simulated CTL production of the cytokine IFN $\gamma$  in order to explore how an antiproliferative effect of IFN $\gamma$  might aid CTLs in tumor control. In this model, IFN $\gamma$  substantially reduced tumor growth compared with direct killing alone. Collectively, these data demonstrate that contact-dependent killing is insufficient for EL4 regression *in vivo* and highlight the potential importance of cytokine-induced antiproliferative effects in T-cell-mediated tumor control.

**Significance:** Computational modeling highlights the importance of cytokine-induced antiproliferative effects in T-cell-mediated control of tumor progression.

## Introduction

In the last decade, immunotherapies for cancer have moved into the mainstream of clinical oncology. Antibodies targeting immune checkpoints have been particularly successful, offering significant advantages over chemotherapy in a range of advanced metastatic, relapsed, and refractory solid tumors. CTLA-4, PD-1, and PD-L1 inhibitors are now approved in melanoma, non-small cell lung cancer, renal cell carcinoma, urothelial carcinoma, merkel cell carcinoma, and some colon cancers (1). Another promising immunotherapeutic approach has been the transfer of large numbers of cytotoxic T lymphocytes (CTL). The transferred cells can be either autologously derived tumor-infiltrating lymphocytes (TIL), or engineered with a chimeric antigen receptor (CAR) for tumor specificity. Note that 2017 saw the first FDA approvals of CAR T cells for treatment of B-cell malignancies (2). The potential of adoptive transfer therapies for solid tumors has been highlighted in trials using TILs against melanoma (3–5), or

CAR T cells against a range of solid tumors (6–8). However, these promising early results have so far failed to transfer into the clinic.

Many attempts are being made to improve the efficacy and broaden the scope of cancer immunotherapies. For example, immunotherapies can have a synergistic effect when applied together with other immunotherapies (9, 10), or with traditional treatments such as radiotherapy and chemotherapy (11, 12). Optimal treatment scheduling and dosages are yet to be determined. Given the danger of life-threatening immune-related adverse events following immunotherapy as well as the high costs involved, biomarkers to indicate which patients are likely to benefit from these treatments will be highly valuable. In particular, the immunosuppressive microenvironment, which often characterizes solid tumors, represents a significant hurdle to the expansion and improvement of immunotherapies. Given the complex nature of the various mechanisms of interaction involved in determining the success of immunotherapies, a quantitative understanding of the contribution of these various mechanisms will be highly beneficial for the rational design and optimization of cancer immunotherapies.

One highly relevant topic requiring greater quantitative insight regards the mechanisms employed by CTLs to control tumors *in vivo*. Indeed, these cells are key players in antitumor immune responses, which they are thought to achieve through being extremely efficient killers. This reputation has primarily been established by *in vitro* studies showing evidence of serial or simultaneous killing of several target cells in a short time frame (13, 14). Killing by CTLs is usually considered to be "direct," i.e., contact dependent, and mediated by either perforin and granzymes, or FAS-L. Several studies have suggested that direct lysis of tumor cells by CTLs is extremely important in tumor

Division of Drug Discovery and Safety, Leiden Academic Centre for Drug Research, Leiden University, Leiden, the Netherlands.

**Note:** Supplementary data for this article are available at Cancer Research Online (<http://cancerres.aacrjournals.org/>).

**Corresponding Author:** Joost B. Beltman, Leiden University, Einsteinweg 55, Leiden 2333 CC, the Netherlands. Phone: 31715274323; E-mail: [j.b.beltman@lacdr.leidenuniv.nl](mailto:j.b.beltman@lacdr.leidenuniv.nl)

Cancer Res 2019;79:3406–16

doi: 10.1158/0008-5472.CAN-18-3147

©2019 American Association for Cancer Research.

control (15–18). However, the reported killing rates of CTLs *in vivo* are typically low (19), and it is not clear whether these rates are indeed sufficient for control of tumors. Several studies have highlighted the importance of "indirect" effects of cytokine signaling by activated T cells in the control of tumors, in particular IFN $\gamma$  (20, 21). IFN $\gamma$  may control tumors by exertion of an antiproliferative effect (22), sensitization of tumor cells to FasL-mediated death (23), recruitment of effector cells of the innate immune system (24), and by causing widespread necrosis of tumor cells along with tumor vasculature destruction (25).

In the current study, we quantitatively compare the importance of direct, contact-dependent killing, with indirect cytokine-mediated tumor control, based on published experiments in which EL4/EG7 tumor cells were infused into mice (18). We chose to focus on the EL4 tumor cell line, which, along with its transformed Ova antigen-expressing derivative EG7, has been widely used to explore the antitumor activities of CTLs in an *in vivo* setting (18, 21, 26–29). Using these cell lines, evidence has emerged supporting an important role for IFN $\gamma$  in tumor control by CTLs, yet a negligible role for direct killing, along with apparently contradictory evidence suggesting an important role for direct killing. Hollenbaugh and colleagues (30) transferred perforin- and FasL-deficient T cells into EG7 tumor-bearing mice, and these deficient T cells were able to control tumors almost as well as their wild-type counterparts. However, IFN $\gamma$ -deficient T cells displayed a marked reduction in tumor control, suggesting that IFN $\gamma$  rather than direct cytotoxicity was the primary mechanism used by CTLs to control the tumor. In contrast, Breart and colleagues (18) used intravital two-photon imaging to show that apoptotic events almost exclusively occurred when tumor cells were contacted by T cells, thus arguing for a major role of direct cytotoxicity. Moreover, they generated mixed tumors, comprising both Ova-expressing EG7 cells and non-Ova-expressing EL4 cells. In these mixed tumors, only the antigen-expressing EG7 cells were eliminated, arguing against an indiscriminate effect from IFN $\gamma$ . We integrate the data acquired at various levels into both an ordinary differential equation (ODE) model and a spatial agent-based model (ABM). Applying these models to the *in vivo* data, we show that the observed T-cell densities and slow killing rate were insufficient to explain the population-level tumor regression observed in the mice. We found that an antiproliferative effect mediated through IFN $\gamma$  signaling allowed CTLs to influence far more cells than direct killing alone, therefore leading to a substantially greater impact on tumor progression. Our modeled scenario corroborated the notion that IFN $\gamma$  plays a crucial role in EL4 tumor control, and reconciles this with the apparently conflicting observation of low reported killing rates and density of infiltrating CTLs.

## Materials and Methods

### Data interpretation

Because the main aim of this work is to test whether CTLs could have controlled the tumor through the sole means of direct killing, we favored "optimism" from the CTL viewpoint wherever the *in vivo* dataset was ambiguous. Thus, we chose model assumptions that promoted tumor control through direct CTL killing. Model parameters are summarized in Table 1.

**Tumor cells.** Tumor volume measurements in the absence of CTL transfer were used to fit the growth rate of both our ODE model

and ABM. Based on manual counting of the images, we estimated that the density of tumor cells was approximately  $10^6$  cells  $\text{mm}^{-3}$ . This value is the default used in all our models. Moreover, Breart and colleagues (18) used flow cytometry to estimate the absolute number of tumor cells inside two tumors 10 days after inception (in the absence of infused T cells). An average of  $4 \times 10^6$  cells were recovered, at a time point where the average tumor volume was approximately  $17 \text{ mm}^3$ , corresponding to a density of approximately  $0.25 \times 10^6$  cells  $\text{mm}^{-3}$ . Given that a substantial fraction of tumor cells were likely lost during the cell isolation procedure (31), this can be viewed as an absolute underestimate of the tumor cell density. To convert between tumor volume and number of tumor cells, we consider direct proportionality between these quantities.

Dead tumor cells are not recognized by CTLs in our models yet are not immediately removed from the models. Parnaik and colleagues (32) found that cultured rat cerebellar neurons were completely cleared within 3 hours of apoptosis by professionally phagocytic microglia, whereas the same cells were incompletely cleared after 9 hours by nonprofessionally phagocytic epithelial cells. We therefore considered tumor cells to persist for an average of 6 hours after apoptosis. Because the number of CTLs in our modeled tumors is proportional to the tumor volume (the sum of numbers of dead and alive cells), inclusion of dead tumor cells increases the ratio of effector:alive target (E:T ratio) and thereby increases the total killing rate.

**CTLs.** Breart and colleagues (18) transferred CTLs to mice on day 5 after tumor injection. Before this point, we consider CTLs to be absent from the tumor. Because killing undertaken by any endogenous CTL should also occur in the control tumors where no CTLs were transferred, this is already accounted for in our fit to the tumor growth data in the absence of CTLs. Breart and colleagues (18) measured the density of CTLs within the tumor on days 7 ( $12,500$  CTLs  $\text{mm}^{-3}$ ) and 8 ( $25,000$  CTLs  $\text{mm}^{-3}$ ). Based on our estimate of  $10^6$  tumor cells  $\text{mm}^{-3}$ , this corresponds to an E:T ratio of 1:80 on day 7, and 1:40 on day 8. Due to the temporally sparse measurements, the exact dynamics of T-cell infiltration into the tumor are not known, and for simplicity, we linearly interpolated between the available data points. Beyond day 8, further data on the density of infiltrating CTLs were not recorded. In reality, T-cell numbers likely peak and then decline a few days after adoptive transfer (22), and T cells often suffer from exhaustion after extended time in the tumor (33, 34). However, it is certainly possible that CTL numbers continued to increase beyond day 8. In line with our policy of taking the most optimistic assumptions from the CTL viewpoint, we considered the ratio of effector T cells to total tumor cells (effector:tumor-cell ratio) to continue to linearly increase after day 8. Also in line with our policy, we do not consider CTLs to diminish in effector function over time (which would make it more difficult to control the tumor). CTLs kill tumor cells at a default rate of  $k = 4 \text{ CTL}^{-1} \text{ day}^{-1}$ .

### ODE model

**Model setup.** ODE simulations were performed in the R language, using the package "deSolve 1.14." Models were fitted using the Levenberg–Marquardt algorithm in the package "minpack.lm 1.2-1." Our ODE model was designed to test whether CTLs could control tumors with the observed direct killing rate of  $k = 4$  kills  $\text{CTL}^{-1} \text{ day}^{-1}$ . Therefore, we deliberately simplified the

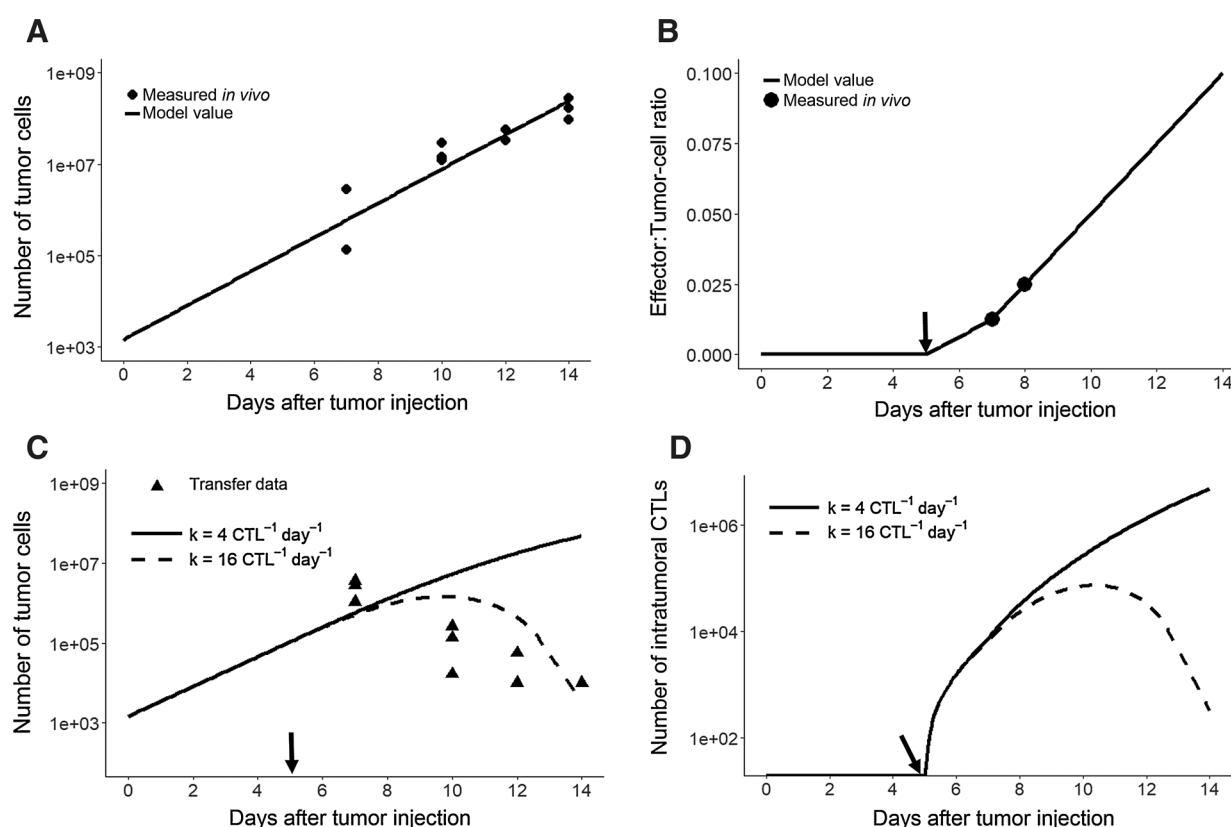


**Figure 1.**

ODE model suggests direct T-cell cytotoxicity is insufficient for control of EG7 tumors. **A**, Tumor growth is described as exponential growth ( $g = 0.86 \text{ day}^{-1}$ ). **B**, effector:tumor-cell ratio in the ODE model is estimated by linear interpolation of measured data points. After day 8, we assume a linear increase in CTL density. **C**, ODE simulation of tumor dynamics in the presence of actively killing CTLs, with two different killing rates. Lines represent model fits, and dots represent experimental data. **D**, Total number of CTLs in simulations with killing. Arrows in **B–D** indicate time of CTL transfer.

model, with assumptions chosen to maximize the likelihood of tumor control. The model consists of two coupled equations:

$$\frac{dT}{dt} = gT - kE(t), \quad (\text{A})$$

$$\frac{dD}{dt} = kE(t) - dD, \quad (\text{B})$$

Thus, tumor cells  $T$  are considered to grow exponentially with rate  $g$  ( $\text{day}^{-1}$ ) in the absence of CTLs, because the experimental tumors clearly did not yet suffer from competition for resources during the measurement interval (Fig. 1A). Tumor cells are killed at rate  $k$  ( $\text{CTL}^{-1} \text{ day}^{-1}$ ) by a population of effector cells  $E(t)$ , where  $E(t)$  is determined based on the number of dead and alive tumor cells (Data Interpretation, Fig. 1B):

$$E(t) = \lambda(T + D) \begin{cases} 0 & \text{if } (t \leq 5) \\ (t - 5) & \text{if } (5 < t \leq 7) \\ 2(1 + (t - 7)) & \text{if } (7 < t), \end{cases} \quad (\text{C})$$

with the parameter  $\lambda$  arising from interpolation of the data ( $\lambda = \frac{1}{160} \text{ cell}^{-1} \text{ day}^{-1}$ ), which defines the rate of increase in the effector:tumor-cell ratio  $E : (T + D)$ .

Killed cells  $D$  are cleared at rate  $d$  ( $\text{day}^{-1}$ ). We took the killing rate to be proportional to the number of CTLs and independent of

the number of target cells, implying that CTLs are considered to always kill at their maximal rate. In reality, a dual saturation function, with saturation in both effector and tumor cell number  $T$ , is a more complete description of CTL killing (Supplementary Methods; refs. 35, 36). However, we aimed to model a situation that favors CTL control of the tumor. In such a best-case scenario from the CTL viewpoint, CTLs always have sufficient targets to kill and need never search for targets. As such our simplified ODE model is an extremely optimistic scenario from the point of view of the CTLs. This simplification implies that our model is a good approximation as long as the E:T ratio remains sufficiently low.

## ABM

**Model setup.** ABM simulations were implemented in C++14, using boost 1.69.0. Visualizations were rendered in C++ using VTK 8.0. We use an asynchronously updating ABM to simulate tumor growth, T-cell infiltration and migration, and tumor regression. Our ABM features two types of agents: CTLs and tumor cells. Tumor cells live on a regular 3D lattice where each cell occupies a single lattice site; tumor cells do not share sites with each other. Empty sites in the lattice represent extracellular matrix, or other cell types not interfering with the tumor. Lattice sites have length of  $10 \mu\text{m}$  by default, roughly corresponding to our default tumor cell density assumptions. Each tumor cell grid point contains

information on the tumor cell type (either EG7 or EL4), the amount of damage it has sustained from CTL attacks, and whether it is alive or not. Throughout the simulation, we track the displacement of the furthest tumor cell from the center of the lattice; this measurement is used to dynamically adjust the size of the simulation domain. The domain is a sphere, extending from the lattice center out to a radius 5 lattice sites (50  $\mu\text{m}$ ) beyond the displacement of the furthest tumor cell.

**Tumor cell behavior.** The tumor is initialized on day 0, by filling  $T_0$  lattice sites with tumor cells within a radius of  $R_i$  from the lattice center. The simulation is advanced in timesteps of 1 minute ( $\Delta t$ ). At each timestep, each tumor cell is liable to replicate with probability  $g\Delta t$ . Cells replicate into a random neighboring square if one is available. We implemented short-range dispersal (similar to ref. 37) as a computationally inexpensive means to achieve exponential, spheroidal tumor growth while comfortably allowing simulation of over  $10^8$  individual agents. Candidate dividing cells whose surroundings are fully occupied attempt to disperse from the tumor with probability  $p_{disp}$ . Dispersing cells produce a daughter cell for which a new location is chosen based on a random walk with mean dispersal distance proportional to the current tumor radius. If the chosen site is vacant, the daughter cell occupies this site, otherwise the dispersal attempt fails.

**CTL infiltration.** CTLs are associated with a location corresponding to a grid site; however, they are not explicitly represented on the grid and as such can share space with other CTLs or tumor cells. Thus, CTLs do not contribute to the tumor mass and are able to move through tumor tissue, attempting to form conjugates with antigen-expressing tumor cells. We allowed for such co-occupancy because CTLs can easily move in between other cells in densely packed environments, such as a lymph node (38) or the skin epidermis (39), and are able to cooperate to kill individual targets (19). Because of the relatively low effector:tumor-cell ratios observed in the experimental data, in practice our CTLs rarely share lattice sites. Specifically, two or more CTLs share a lattice site only approximately 2% of the time, and 3 or more share a site only approximately 0.01% of the time on day 8 of a typical simulation. Following the experimental setup, CTLs infiltrate the tumor on day 5 after tumor inception. New CTLs arrive at random points within the existing simulation domain. At each timestep, a target number of CTLs is calculated based on the effector:tumor-cell ratio we estimated from the data (in equivalence with the ODE model). If the number of CTLs inside the simulation is below the current target, new CTLs are added to the simulation until the target is reached. CTLs are only removed from the simulation when they migrate outside the simulation domain. The number of CTLs may therefore exceed the target density, albeit only while the tumor disappears more quickly than CTLs migrate out of the simulation domain.

**CTL migration.** CTLs migrate until they reach a site occupied by a tumor cell; CTLs that migrate outside the simulation domain are removed. Although a CTL is migrating, each timestep, it randomly moves to an adjacent lattice site within its 3D Moore neighborhood including its current location. Thus, there is a  $1/27$  probability of no movement, a  $6/27$  probability of a  $10\mu\text{m}$  movement,  $8/27$  probability of a  $10\sqrt{2}\mu\text{m}$  movement, and a  $8/27$  probability of a  $10\sqrt{3}\mu\text{m}$  movement. Therefore, the resulting migra-

tion speed is  $11.5\mu\text{m}$  per minute, which is in close agreement with previously measured values in the EL4/EG7 tumor (29). CTLs that find tumor cells arrest with probability  $p_{arr}$ , and subsequently attack tumor cells with probability  $p_{hit}$  or detach and resume migration with probability  $p_{det}$ . By default,  $p_{arr} = 1$  and  $p_{det} = 0$ , although these are varied to  $p_{arr} = 0.9$  and  $p_{det} = 0.01$  in the simulations where we examine multihitting CTL. CTLs are immediately released from conjugates if the target cell dies.

**Effects of CTLs on tumor cells.** Tumor cells may sustain  $n_{hit}$  hits from CTLs before apoptosis occurs. By default,  $n_{hit} = 1$ , in which case, CTLs attack targets with an attack rate identical to the killing rate. In simulations where multiple hits are required for tumor cell death, the base attack rate is multiplied by the number of hits required for apoptosis. Therefore, the overall killing potential of the CTLs is controlled between single-hit and multiple-hit simulations to obtain equal killing rates.

In simulations with IFN $\gamma$ , that cytokine is produced at a constant rate by CTLs while conjugated with tumor cells. IFN $\gamma$  is consumed by tumor cells, and tumor cells cannot divide when the local IFN $\gamma$  concentration exceeds a threshold value. We set the diffusion parameters such that the threshold occurs at around 3-cell lengths away from a conjugated CTL. For details, see the Supplementary Methods.

**Mixed tumors.** We simulated mixed EL4/EG7 tumors by seeding a 50/50 mixture of cells on day 0. The only difference between these cell types is that EG7 cells are not recognized by CTLs.

## Results

### Direct CTL cytotoxicity is not sufficient to mediate *in vivo* regression of EG7 tumors

In the *in vivo* data of Breart and colleagues (18), transferred OTI effector T cells rapidly controlled an infused EG7 tumor, following direct contact with tumor cells. However, each infiltrating CTL killed on average only 4 tumor cells per day, and it is unclear if tumor regression should be expected based on the density and cytotoxic activity observed in this *in vivo* data. To test whether CTLs could reasonably be expected to control the *in vivo* tumors, we employed an ODE model (see Materials and Methods) that integrated the measurements made at various levels. Instead of providing a detailed description of the tumor and its interactions with the immune system, the goal of this model was rather to assess the possibility that direct killing could have solely accounted for tumor regression. The simplifications that we made in the ODE model always favored the CTLs, i.e., they made tumor regression more likely. If indeed CTLs were capable of controlling the tumor by direct killing alone, tumor regression would certainly be observed in this simplified model.

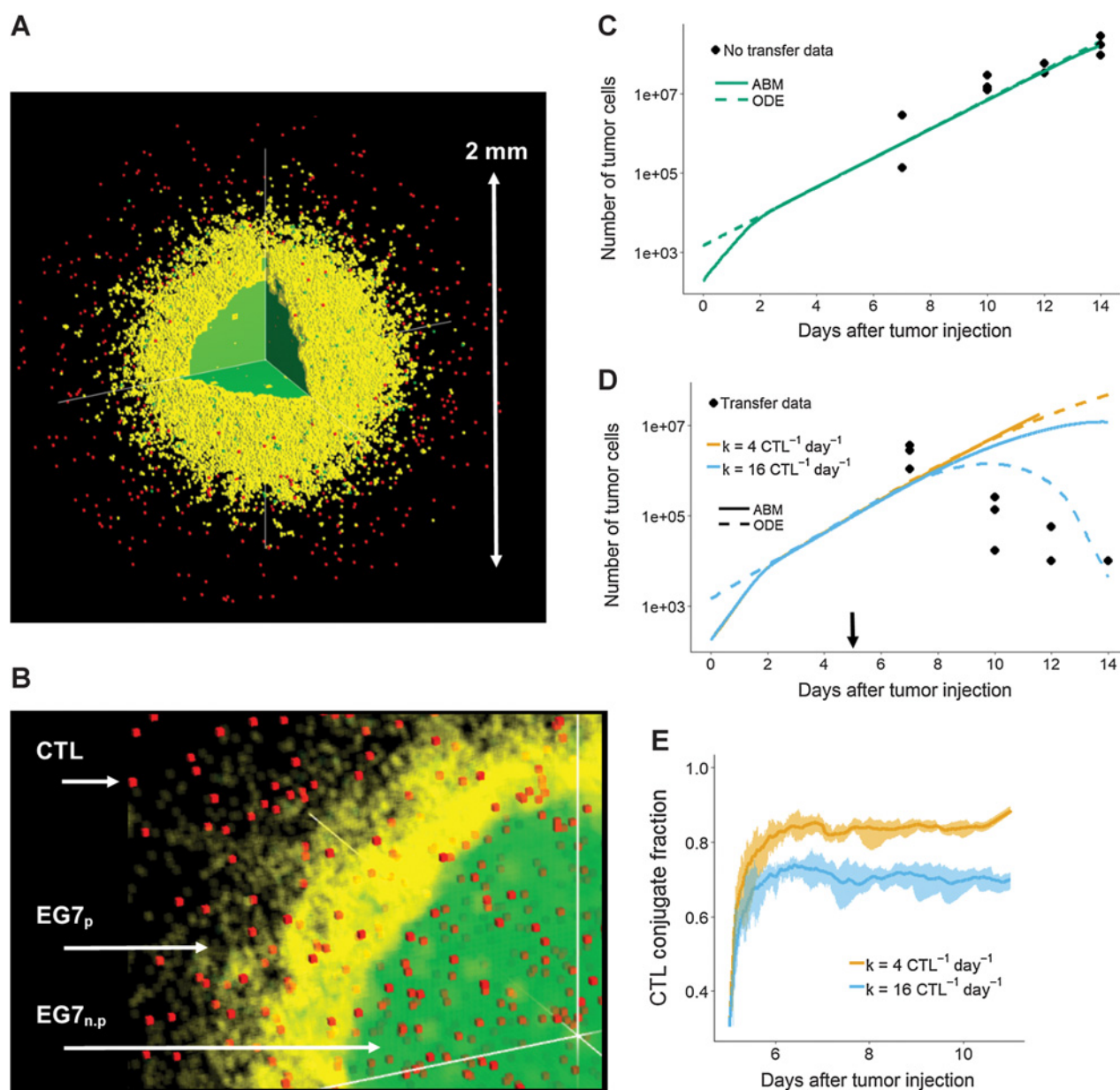
Modeling tumor growth as an exponential process resulted in a good match to the tumor measurements from Breart and colleagues (18) for the case without T-cell transfer (Fig. 1A), suggesting that tumor growth was not yet inhibited by factors such as competition for nutrients. Subsequently, we introduced a population of CTLs into this model, with effector:tumor-cell ratio based also upon experimental measurements (Fig. 1B). The impact on the tumor was limited when CTLs killed tumor cells at a rate of  $k = 4\text{ CTL}^{-1}\text{day}^{-1}$  as reported by Breart and colleagues (Fig. 1C; ref. 18), despite the continuous increase in intratumoral T-cell numbers (Fig. 1D). The killing rate measurements were

relatively uncertain compared with the other parameters in the ODE model, perhaps having varied over time or throughout the tumor. To address that uncertainty, we simulated CTL populations killing with rate up to  $k = 16 \text{ CTL}^{-1} \text{ day}^{-1}$ , which is at the high end of the range of reported estimates for CTL killing performance *in vivo* (40). As a side note, in this model, such a 4-fold increase of the killing rate is equivalent to a 4-fold increase of the CTL infiltration rate. With  $k = 16$ , our simulated tumors were controlled, although this control occurred only at much later time points than was the case for the *in vivo* tumors. Thus, even for

the extremely optimistic scenario we consider and using a substantially higher killing rate than was measured experimentally, direct CTL lysis alone could not explain the observed *in vivo* tumor regression.

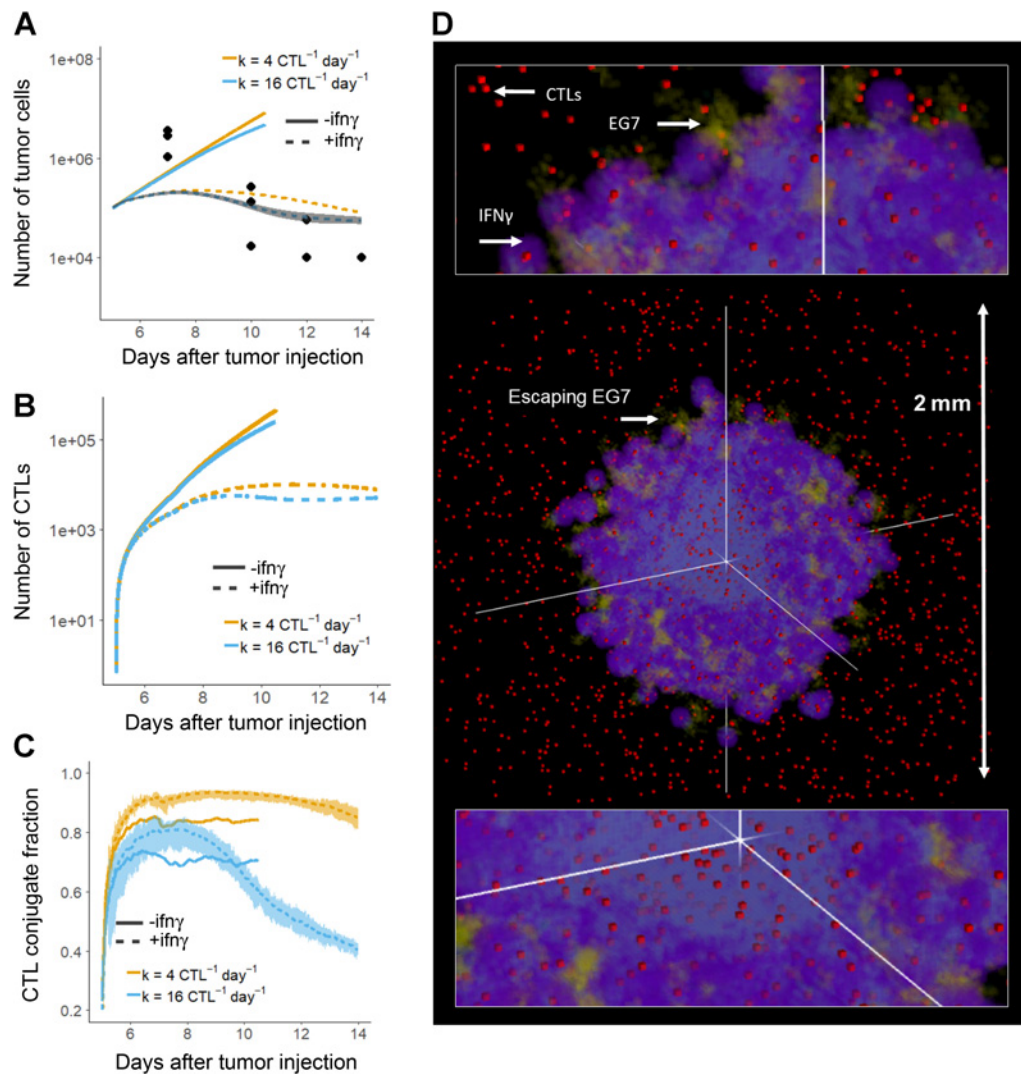
#### ABM supports notion that CTL cytotoxicity is insufficient to mediate *in vivo* regression of EG7 tumors

We developed a spatially explicit ABM with tumor cells and CTLs as agents to contrast against the idealized ODE model (Fig. 2A and B). As in the ODE model, in the ABM the overall



**Figure 2.**

ABM confirms that direct T-cell cytotoxicity is insufficient for control of EG7 tumors. **A** and **B**, ABM tumor infiltrated by CTLs on day 7. EG7 with free adjacent lattice sites can proliferate (EG7<sub>p</sub>). EG7 with no free adjacent lattice sites are nonproliferating (EG7<sub>n.p</sub>), although they may still disperse (see Materials and Methods). **C** and **D**, Comparison of tumor evolution in ABM (solid lines) and ODE model (dashed lines) without (**C**) and with (**D**) transferred CTLs, where arrow indicates time of CTL transfer. **E**, Fraction of CTLs in a conjugate with a tumor cell throughout ABM simulations.

**Figure 3.**

Antiproliferative IFN $\gamma$  leads to tumor control. **A**, Simulated tumor volume compared with and without IFN $\gamma$ -producing CTLs. **B**, Total CTL numbers in simulations with or without IFN $\gamma$ . **C**, Fraction of CTLs in conjugates in simulations with and without IFN $\gamma$ . **D**, Tumor on day 8, in the presence of IFN $\gamma$ .

growth rate of the tumor was matched to the data in the absence of CTLs (Fig. 2C), although the ABM differs in that tumor cells cannot divide when fully surrounded, i.e., there is competition for space (Supplementary Video S1). Tumors were much less well controlled in the ABM than they were in the ODE model (Fig. 2D); even at a killing rate of  $k = 16 \text{ CTL}^{-1} \text{ day}^{-1}$ , the tumor was not controlled in the ABM. There are two reasons for this discrepancy. First, when compared with the ODE model, the ABM has the added requirement that CTLs must migrate in order to find tumor cells to kill. Indeed, the fraction of CTLs in conjugates was lower in simulations with  $k = 16 \text{ CTL}^{-1} \text{ day}^{-1}$  than in those with  $k = 4 \text{ CTL}^{-1} \text{ day}^{-1}$  (Fig. 2E), because faster killing CTLs spend less time conjugated with tumor cells. The second source of discrepancy between the ODE and ABM results stems from the competition for space between tumor cells that occurs in our ABM; CTL killing eases such competition, so tumor control is more difficult. Thus, the idealized ABM highlights that CTLs might make their own job more difficult by being highly efficient killers. Overall, the ABM

simulations confirm that CTL-mediated direct killing alone cannot explain EG7 tumor regression.

#### IFN $\gamma$ -mediated cell-cycle arrest is sufficient for tumor control

Because IFN $\gamma$  has been widely implicated in tumor eradication (20–25), we added production and diffusion of this cytokine to our ABM. We focused on an antiproliferative effect of IFN $\gamma$  because Breart and colleagues (18) only detected apoptosis in tumor cells directly contacted by CTLs, an observation that is inconsistent with the notion of significant IFN $\gamma$  cytotoxicity toward EG7 cells. To test the contribution of the putative antiproliferative effect of IFN $\gamma$ , we simulated tumors with  $k = 4 \text{ CTL}^{-1} \text{ day}^{-1}$  or  $k = 16 \text{ CTL}^{-1} \text{ day}^{-1}$ , in the presence or absence of IFN $\gamma$ . In our simulated tumors, the antiproliferative effect of IFN $\gamma$  was much stronger than the contact-dependent CTL lysis, even with  $k = 16 \text{ CTL}^{-1} \text{ day}^{-1}$  (Fig. 3A). Although tumors were rapidly controlled in our model with IFN $\gamma$ , they were not entirely eradicated. This can be explained by the low number of CTLs in

the IFN $\gamma$  simulations (Fig. 3B), together with the fraction of conjugated CTLs, which drops after the onset of tumor regression for  $k = 16 \text{ CTL}^{-1}\text{day}^{-1}$  (Fig. 3C). CTLs mostly eradicate tumor cells in the center of the spheroid, but some pockets of tumor cells in the periphery survive and allow the tumor to escape (Fig. 3D; Supplementary Video S2). These modeled behaviors are consistent with literature observations that solid tumors "melt from the inside" (41), and that EL4 tumors may rebound after an initial response to transferred CTLs (42). In summary, tumor cell-cycle arrest due to cytokine production by CTLs in addition to their cytotoxicity can explain the observed response of EG7 cells to a population of transferred CTLs.

### CTL cooperativity leads to heterogeneity in killing rate

Our ABM predicted an almost negligible role for direct killing in tumor regression, with or without the presence of IFN $\gamma$ . However, the CTL killing rate may in reality have been higher than the measured  $k = 4 \text{ CTL}^{-1}\text{day}^{-1}$  and may not have been constant over time (36). Factors that could play a role here include the ability of CTLs to kill collaboratively (19) and that of cancer cells to resist multiple CTL "hits" before apoptosis is triggered (43). We therefore used our ABM to assess whether the measurement of  $k = 4 \text{ CTL}^{-1}\text{day}^{-1}$  could have resulted from a higher "intrinsic" CTL killing rate. We compared simulations in which tumor cells die after a single "lethal hit" with simulations where an accumulation of several hits was required for apoptosis. There was no substantive difference between the single-hit and multihit scenarios in terms of tumor growth (Fig. 4A), or number of CTLs (Fig. 4B). At early time points, the fraction of CTLs in conjugates in the multihit model was slightly higher than in the single-hit model (Fig. 4C), and the temporal pattern of killing rate per simulated CTL (Fig. 4D) or per conjugated CTL (Fig. 4E) differs between the two settings. Multihitting CTL populations initially killed at a low rate, because targets had generally not acquired enough damage to die. Subsequently, targets accumulated damage, and the manifested killing rate per conjugated CTL rose above the killing rate for the single-hit scenario (Fig. 4E). Similar to the killing rate measurement procedure of Breart and colleagues (18), we measured killing in  $100 \mu\text{m} \times 100 \mu\text{m} \times 30 \mu\text{m}$  "windows" for a 2-hour period at the beginning of day 8 during a cumulative total of 75 hours of conjugated CTL imaging time (18). Our analysis shows that such sample sizes in general reflect the global killing rate well (Fig. 4F). As a side note, in our model, the infiltration of the tumors by CTLs was relatively homogeneous, meaning that damage to targets occurred roughly evenly throughout the tumor (Fig. 4G). Although heterogeneous infiltration may lead to strong spatial variability in killing rate, we conclude that temporal variation in killing is likely large, especially when CTLs cooperate.

### Direct killing plus antiproliferative IFN $\gamma$ accounts for selective elimination of antigen-positive cells

Breart and colleagues (18) noted that in mixed EL4/EG7 tumors, the non-cognate antigen-expressing tumor cells (EL4) grew more or less unconstrained, and it is unclear whether the antiproliferative effect of IFN $\gamma$  is consistent with this finding. We therefore simulated mixed tumors, containing patches of antigen-positive EG7 cells or antigen-negative EL4 cells. EL4 cells were considered not to be recognized and thus not affected by direct interactions with CTLs, but could be affected by IFN $\gamma$  that diffused from nearby locations. When initialized with a 50% mixture of EL4/EG7 cells, our simulated tumors form patches with similar

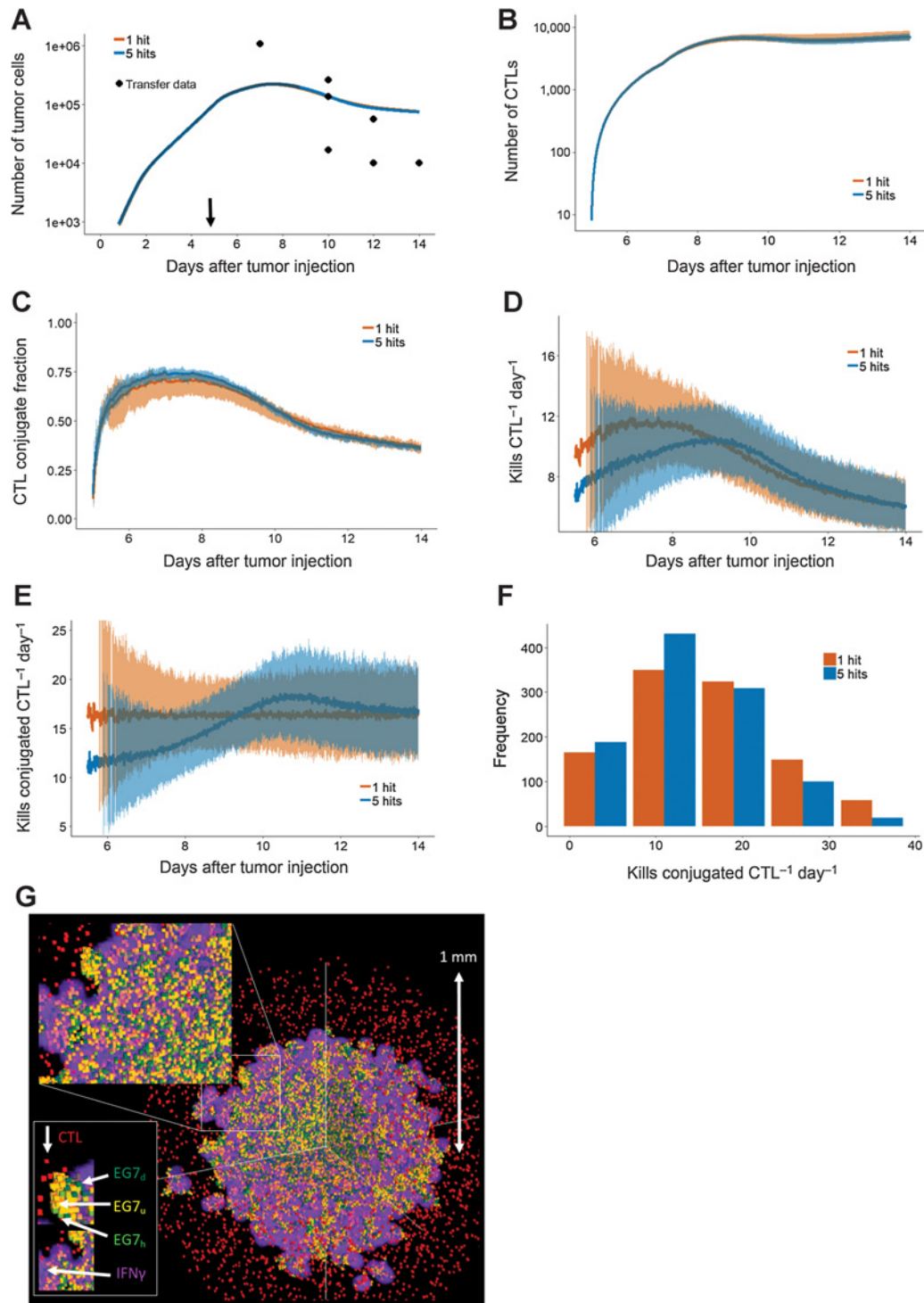
spatial dimensions to the images from Breart and colleagues (Fig. 5A). We simulated the transfer of CTLs into the mixed tumor model, upon which CTLs preferentially accumulated in regions of Ova-expressing EG7 cells where they began killing these cells and secreting IFN $\gamma$  (Fig. 5B; Supplementary Video S3). IFN $\gamma$  concentrations were generally higher in regions of EG7 cells compared with regions of EL4 cells, yet despite the limited ( $\sim 30 \mu\text{m}$ ) range of IFN $\gamma$  diffusion in our model, many EL4 cells were prevented from replicating for a period of approximately 2 days, when the activity of the CTLs was greatest (Fig. 5C). By day 10, most EG7 cells were eliminated, and the CTLs, being deprived of stimulation, stopped producing IFN $\gamma$ . After this point, EL4 cells resumed growth, eventually filling the spaces left behind by the dead EG7 cells. EL4 cells were thus not so much affected by the presence of the CTLs. In conclusion, local production of antiproliferative IFN $\gamma$  is consistent with the experimental observation that within mixed tumors primarily cognate antigen-expressing cells were cleared by CTLs.

## Discussion

Immunotherapies involving CTLs are able to mediate regression or tumor control in cancers that were previously out of reach for conventional treatments. Despite major progress, many patients fail to respond, and the mechanistic insight required to explain this disparity in outcomes is lacking. Lysis of infected or malignant cells following direct physical contact is the canonical CTL effector function, but indirect effects of CTLs such as production of cytokines are increasingly recognized as having an important role in CTL-mediated tumor regression (21, 22, 25, 44). The relative importance of these different mechanisms remains unclear and is likely to depend on characteristics of both the tumor and the T cells involved. Here, we developed an ABM and an ODE model of tumor regression following adoptive transfer of a population of CTLs attacking EL4/EG7 tumor cells. Using these models, we attempted to quantify the relative contribution of direct CTL killing toward tumor regression in the EL4/EG7 model. Our simulated tumors were not controlled by direct CTL killing only, so we conclude that direct killing was not a sufficient explanation for regression in the EL4 tumor model.

In our ABM, we also included simulation of an antiproliferative effect of IFN $\gamma$ , because Hollenbaugh and colleagues (21) observed that IFN $\gamma$ -deficient T cells display substantially reduced tumor controlling abilities. We modeled an antiproliferative effect because the tumor cells were only observed to die after CTL contact, evidence against a substantial long-distance cytotoxic effect of IFN $\gamma$  in this *in vivo* setting. IFN $\gamma$  secreted by CTLs has been shown to contribute to regression in a different tumor model (22), by arresting the cell cycle of tumor cells. Although IFN $\gamma$  has no direct antiproliferative effect on EL4 cells *in vitro* (22), it has been shown that nitric oxide (NO) is secreted by stromal cells after exposure to IFN $\gamma$  (21). Such NO reduces proliferation of EL4 cells *in vitro* (21), and thereby provides a possible mechanism for the growth inhibition included in our model. Note that we incorporated a direct effect of IFN $\gamma$  on tumor proliferation rather than explicitly including this potential cascade of events, because detailed quantitative measurements on these mechanisms are currently lacking.

Although the antiproliferative effect of IFN $\gamma$  may be an important contributor to tumor control, IFN $\gamma$  may have had other effects that we did not take into account. First, although we were able to

**Figure 4.**

T-cell cooperativity causes heterogeneity in killing rate. **A–E**, Comparison of simulated tumor volume (**A**), total number of CTLs (**B**), fraction of conjugated CTLs (**C**), killing rate per simulated CTL (**D**), and killing rate per conjugated CTL (**E**) between simulations, where CTLs required 1 or 5 hits to kill targets, in the presence of IFN $\gamma$ . Arrow in **A**, CTL transfer. **F**, Killing rate measured from 2-hour windows beginning on day 8. **G**, Distribution of dead (EG7<sub>d</sub>), damaged ("hit," EG7<sub>h</sub>), or healthy ("unhit," EG7<sub>u</sub>) tumor cells.

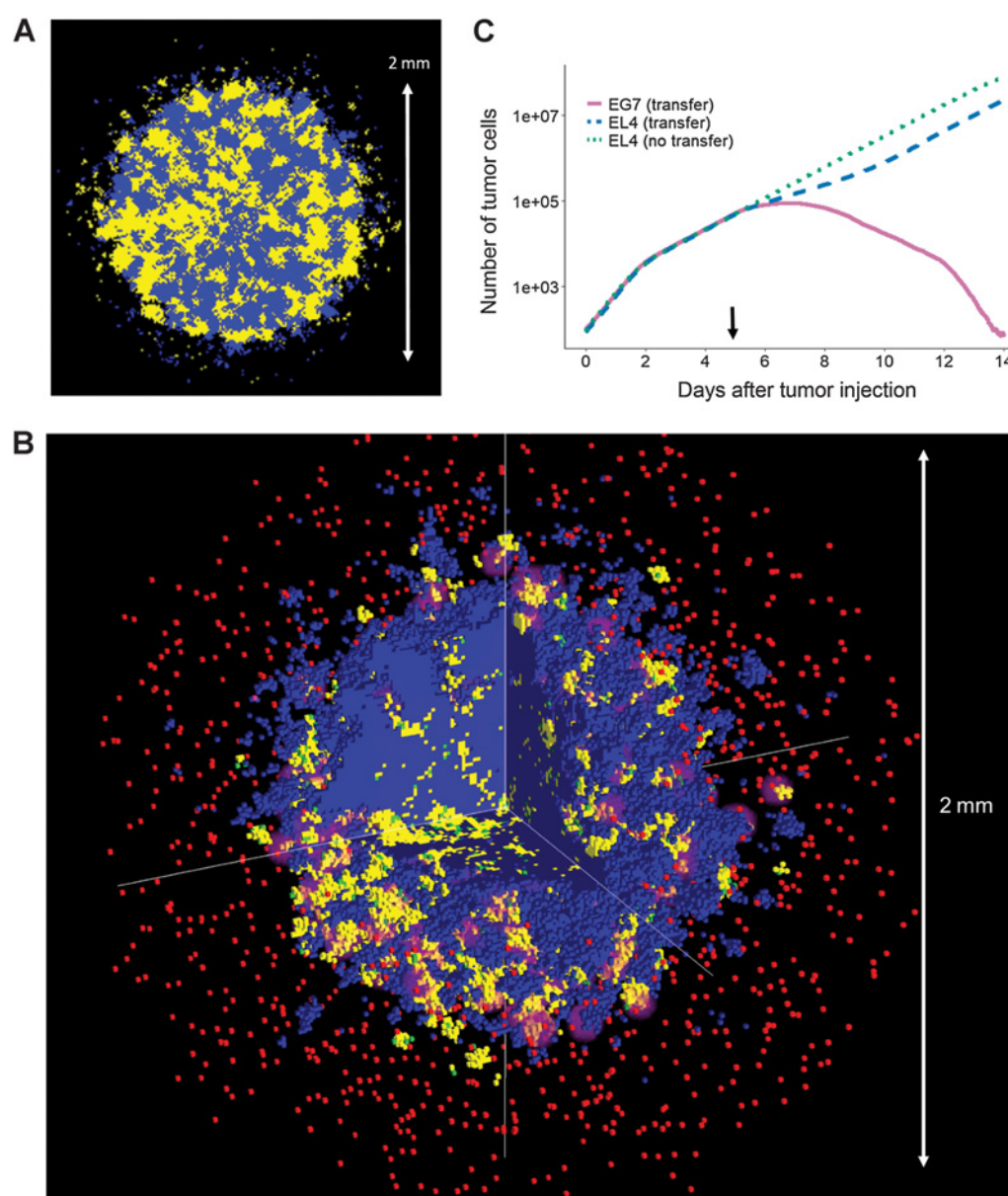


**Figure 5.**

Antiproliferative IFN $\gamma$  explains selective destruction of EG7 cells within EG7/EL4-mixed tumors. **A**, Example 2D slice from the center of a simulated mixed tumor 8 days after tumor inception. **B**, Images showing examples of tumor composition (T cells, red; EG7 cells, yellow; EL4 cells, blue; IFN $\gamma$  concentrations, purple) on day 8 during the course of EG7 regression. **C**, Evolution of the total volume of EG7 or EL4 cells in mixed tumor simulations. Arrow, time of CTL transfer.

explain regression without a substantial cytotoxic effect of IFN $\gamma$ , we cannot exclude that possibility. Because such an effect does not act specifically toward tumor cells presenting cognate antigen, it may be an important mechanism to control antigen loss variants, which might otherwise allow tumors to recur. Second, IFN $\gamma$  may induce immuno-tolerance, leading to decreased CTL effector function (45). Third, it has been speculated that IFN $\gamma$  aids in control of tumors by recruitment of innate effector cells (24), or destruction of tumor vasculature (44). Our model included neither of these effects because they were not apparent in the experiments we based our model on. However, it is possible

that these events happened at a later time, after observations of CTL killing were made. This further underlines that measurements are required throughout the entire course of tumor rejection, in order to gain a full understanding of the sequence of events that occurs.

Apart from the role that IFN $\gamma$  may play in tumor control, our modeling has also highlighted a potential explanation for temporal variation in measured killing rates of CTLs. Tumor cells may be able to endure multiple attacks from CTLs before apoptosis is triggered (19, 43). When we implemented such variability in our model, we indeed found an increase in killing rate over the course

**Table 1.** Overview of parameters used in models, what they represent, and their default value

Parameter	Description	Default value
$T_0$	Number of tumor cells at time 0	1,450 (ODE) 180 (ABM)
$E_0$	Number of CTLs at time 0	0
$D_0$	Number of killed tumor cells at time 0	0
$k$	CTL killing rate	4 kills CTL <sup>-1</sup> day <sup>-1</sup>
$g$	Tumor growth rate	0.86 day <sup>-1</sup> (ODE) 1.97 day <sup>-1</sup> (ABM)
$d^a$	Disappearance rate of killed tumor cells	2 day <sup>-1</sup>
$p_{arr}$	Probability of conjugate formation	1 (ABM)
$n_{hit}^b$	Number of hits before tumor cell apoptosis	1 (ABM)
$p_{det}$	Probability of conjugate splitting	0 (ABM)
$p_{disp}$	Probability of tumor cell dispersal	0.03 (ABM)
$R_i$	Initial tumor radius	120 $\mu$ m (ABM)

NOTE: Parameters apply to ABM and ODE model unless indicated otherwise; parameter values are based on data in Breart and colleagues (18) unless indicated otherwise.

<sup>a</sup>Based on Parnaik and colleagues (32).

<sup>b</sup>Based on Halle and colleagues (19).

of tumor regression. This dependence of killing rate upon measurement time is in agreement with our previous modeling work (36) on T-cell–target cell interactions.

A criticism of our approach could be that our simulations do not capture all the myriad complex interactions within the tumor microenvironment. Indeed, our models are a highly idealized representation of reality, because they contain only the mechanisms we explicitly chose to include. This would likely be a problem if using the model as a fully predictive tool for other settings, because the model predictions will not be valid in tumors where unincluded mechanisms are important. However, when applying the model as a diagnostic tool (as we have here), model simplicity is a major advantage. This approach allowed us to quantitatively test whether observations made at the cellular level could explain emergent behavior of the tumor as a whole, without the interference of confounding variables.

## References

- Jardim DL, de Melo Gagliato D, Giles FJ, Kurzrock R. Analysis of drug development paradigms for immune checkpoint inhibitors. *Clin Cancer Res* 2018;24:1785–94.
- Yip A, Webster RM. The market for chimeric antigen receptor T cell therapies. *Nat Rev Drug Discov* 2018;17:161–2.
- Besser MJ, Shapira-Frommer R, Treves AJ, Zippel D, Itzhaki O, Hershkovitz L, et al. Clinical responses in a phase II study using adoptive transfer of short-term cultured tumor infiltration lymphocytes in metastatic melanoma patients. *Clin Cancer Res* 2010;16:2646–55.
- Rosenberg SA, Yang JC, Sherry RM, Kammula US, Hughes MS, Phan GQ, et al. Durable complete responses in heavily pretreated patients with metastatic melanoma using T-cell transfer immunotherapy. *Clin Cancer Res* 2011;17:4550–7.
- Chandran SS, Somerville RPT, Yang JC, Sherry RM, Klebanoff CA, Goff SL, et al. Treatment of metastatic uveal melanoma with adoptive transfer of tumor-infiltrating lymphocytes: a single-centre, two-stage, single-arm, phase 2 study. *Lancet Oncol* 2017;18:792–802.
- Feng K, Guo Y, Dai H, Wang Y, Li X, Jia H, et al. Chimeric antigen receptor-modified T cells for the immunotherapy of patients with EGFR-expressing advanced relapsed/refractory non-small cell lung cancer. *Sci China Life Sci* 2016;59:468–79.
- Louis CU, Savoldo B, Dotti G, Pule M, Yvon E, Myers GD, et al. Antitumor activity and long-term fate of chimeric antigen receptor-positive T cells in patients with neuroblastoma. *Blood* 2011;118:6050–6.
- Ahmed N, Brawley VS, Hegde M, Robertson C, Ghazi A, Gerken C, et al. Human epidermal growth factor receptor 2 (HER2)-specific chimeric antigen receptor-modified T cells for the immunotherapy of HER2-positive sarcoma. *J Clin Oncol* 2015;33:1688–96.
- Larkin J, Chiarion-Sileni V, Gonzalez R, Grob JJ, Cowey CL, Lao CD, et al. Combined nivolumab and ipilimumab or monotherapy in untreated melanoma. *N Engl J Med* 2015;373:23–34.
- Swart M, Verbrugge I, Beltman JB. Combination approaches with immune-checkpoint blockade in cancer therapy. *Front Oncol* 2016;6:233.
- Pfirschke C, Engblom C, Rickelt S, Cortez-Retamozo V, Garriss C, Pucci F, et al. Immunogenic chemotherapy sensitizes tumors to checkpoint blockade therapy. *Immunity* 2016;44:343–54.
- Weichselbaum RR, Liang H, Deng L, Fu YX. Radiotherapy and immunotherapy: a beneficial liaison? *Nat Rev Clin Oncol* 2017;14:365–79.
- Isaaz S, Baetz K, Olsen K, Podack E, Griffiths GM. Serial killing by cytotoxic T lymphocytes: T cell receptor triggers degranulation, re-filling of the lytic granules and secretion of lytic proteins via a non-granule pathway. *Eur J Immunol* 1995;25:1071–9.
- Wiedemann A, Depoil D, Faroudi M, Valitutti S. Cytotoxic T lymphocytes kill multiple targets simultaneously via spatiotemporal uncoupling of lytic and stimulatory synapses. *Proc Natl Acad Sci U S A* 2006;103:10985–90.
- Kägi D, Ledermann B, Bürki K, Seiler P, Odermatt B, Olsen KJ, et al. Cytotoxicity mediated by T cells and natural killer cells is greatly impaired in perforin-deficient mice. *Nature* 1994;369:31–7.

Our work highlights the need for further investigation of indirect effects mediated by CTLs in an antitumor immune response. Although many mechanisms utilized by CTLs to control tumors have been identified, quantitative measurements detailing their contribution to regression are scarce. Such quantitative understanding would enable a more sophisticated and systems-based understanding of the interplay of various mechanisms in tumor regression following immunotherapy—and likely enable better targeted interventions. Future studies should therefore aim to characterize the potential contribution of various mechanisms to tumor regression. Computational models that integrate *in vitro* and *in vivo* experiments, such as those developed here and as developed by others (46–48), can be a valuable tool to aid in this process.

## Disclosure of Potential Conflicts of Interest

No potential conflicts of interest were disclosed.

## Authors' Contributions

Conception and design: R.J. Beck, J.B. Beltman

Development of methodology: R.J. Beck, M. Slagter

Analysis and interpretation of data (e.g., statistical analysis, biostatistics, computational analysis): R.J. Beck, M. Slagter

Writing, review, and/or revision of the manuscript: R.J. Beck, J.B. Beltman

Study supervision: J.B. Beltman

## Acknowledgments

We would like to thank Beatrice Bréart and Philippe Bousso for providing their previously published data and for useful feedback on our modeling of their data. This work is supported by a Vidi grant from the Netherlands Organisation for Scientific Research (NWO; grant 864.12.013 to J.B. Beltman).

The costs of publication of this article were defrayed in part by the payment of page charges. This article must therefore be hereby marked *advertisement* in accordance with 18 U.S.C. Section 1734 solely to indicate this fact.

Received October 9, 2018; revised February 8, 2019; accepted April 25, 2019; published first April 30, 2019.

16. Smyth MJ, Kershaw MH, Darcy PK, Trapani JA. Adoptive transfer: the role of perforin in mouse cytotoxic T lymphocyte rejection of human tumor xenografts in vivo. *Xenotransplantation* 1998;5:146–53.
17. Caldwell SA, Ryan MH, McDuffie E, Abrams SI. The Fas/Fas ligand pathway is important for optimal tumor regression in a mouse model of CTL adoptive immunotherapy of experimental CMS4 lung metastases. *J Immunol* 2003;171:2402–12.
18. Breart B, Lemaître F, Celli S, Bousso P. Two-photon imaging of intratumoral CD8+ T cell cytotoxic activity during adoptive T cell therapy in mice. *J Clin Invest* 2008;118:1390–7.
19. Halle S, Keyser KA, Stahl FR, Busche A, Marquardt A, Zheng X, et al. In vivo killing capacity of cytotoxic T cells is limited and involves dynamic interactions and T cell cooperativity. *Immunity* 2016;44:233–45.
20. Barth RJ Jr, Mulé JJ, Spiess PJ, Rosenberg SA. Interferon gamma and tumor necrosis factor have a role in tumor regressions mediated by murine CD8+ tumor-infiltrating lymphocytes. *J Exp Med* 1991;173:647–58.
21. Hollenbaugh JA, Dutton RW. IFN- $\gamma$  regulates donor CD8 T cell expansion, migration, and leads to apoptosis of cells of a solid tumor. *J Immunol* 2006;177:3004–11.
22. Matsushita H, Hosoi A, Ueha S, Abe J, Fujieda N, Tomura M, et al. Cytotoxic T lymphocytes block tumor growth both by lytic activity and IFN $\gamma$ -dependent cell-cycle arrest. *Cancer Immunol Res* 2015;3:26–36.
23. Selleck WA, Canfield SE, Hassen WA, Meseck M, Kuzmin AI, Eisensmith RC, et al. IFN-gamma sensitization of prostate cancer cells to Fas-mediated death: a gene therapy approach. *Mol Ther* 2003;7:185–92.
24. Nagoshi M, Sadanaga N, Joo HG, Goedegebuure PS, Eberlein TJ. Tumor-specific cytokine release by donor T cells induces an effective host anti-tumor response through recruitment of host naive antigen presenting cells. *Int J Cancer* 1999;80:308–14.
25. Briesemeister D, Sommermeyer D, Lodenkemper C, Loew R, Uckert W, Blankenstein T, et al. Tumor rejection by local interferon gamma induction in established tumors is associated with blood vessel destruction and necrosis. *Int J Cancer* 2011;128:371–8.
26. Nguyen HH, Kim T, Song SY, Park S, Cho HH, Jung SH, et al. Naïve CD8(+) T cell derived tumor-specific cytotoxic effectors as a potential remedy for overcoming TGF- $\beta$  immunosuppression in the tumor microenvironment. *Sci Rep* 2016;6:28208.
27. Mikucki ME, Fisher DT, Matsuzaki J, Skitzki JJ, Gaulin NB, Muhitch JB, et al. Non-redundant requirement for CXCR3 signalling during tumoricidal T-cell trafficking across tumor vascular checkpoints. *Nat Commun* 2015;6:7458.
28. Yao Y, Chen S, Cao M, Fan X, Yang T, Huang Y, et al. Antigen-specific CD8+ T cell feedback activates NLRP3 inflammasome in antigen-presenting cells through perforin. *Nat Commun* 2017;8:15402.
29. Boissonnas A, Fétter L, Zeelenberg IS, Hugues S, Amigorena S. In vivo imaging of cytotoxic T cell infiltration and elimination of a solid tumor. *J Exp Med* 2007;204:345–56.
30. Hollenbaugh JA, Reome J, Dobrzanski M, Dutton RW. The rate of the CD8-dependent initial reduction in tumor volume is not limited by contact-dependent perforin, Fas ligand, or TNF-mediated cytotoxicity. *J Immunol* 2004;173:1738–43.
31. Steinert EM, Schenkel JM, Fraser KA, Beura LK, Manlove LS, Igyártó BZ, et al. Quantifying memory CD8 T cells reveals regionalization of immunosurveillance. *Cell* 2015;161:737–49.
32. Parnaik R, Raff MC, Scholes J. Differences between the clearance of apoptotic cells by professional and non-professional phagocytes. *Curr Biol* 2000;10:857–60.
33. Hirano K, Hosoi A, Matsushita H, Iino T, Ueha S, Matsushima K, et al. The nitric oxide radical scavenger carboxy-PTIO reduces the immunosuppressive activity of myeloid-derived suppressor cells and potentiates the anti-tumor activity of adoptive cytotoxic T lymphocyte immunotherapy. *Oncoimmunology* 2015;4:e1019195.
34. Pauken KE, Wherry EJ. Overcoming T cell exhaustion in infection and cancer. *Trends Immunol* 2015;36:265–76.
35. Gadamsetty S, Marée AFM, Beltman JB, de Boer RJ. A general functional response of cytotoxic T lymphocyte-mediated killing of target cells. *Biophys J* 2014;106:1780–91.
36. Gadamsetty S, Marée AFM, Beltman JB, de Boer RJ. A sigmoid functional response emerges when cytotoxic T lymphocytes start killing fresh target cells. *Biophys J* 2017;112:1221–35.
37. Waclaw B, Bozic I, Pittman ME, Hruban RH, Vogelstein B, Nowak MA. A spatial model predicts that dispersal and cell turnover limit intratumor heterogeneity. *Nature* 2015;525:261–4.
38. Beltman JB, Marée AFM, Lynch JN, Miller MJ, de Boer RJ. Lymph node topology dictates T cell migration behavior. *J Exp Med* 2007;204:771–80.
39. Ariotti S, Beltman JB, Chodaczek G, Hoekstra ME, van Beek AE, Gomez-Eerland R, et al. Tissue-resident memory CD8+ T cells continuously patrol skin epithelia to quickly recognize local antigen. *Proc Natl Acad Sci U S A* 2012;109:19739–44.
40. Halle S, Halle O, Förster R. Mechanisms and dynamics of T cell-mediated cytotoxicity in vivo. *Trends Immunol* 2017;38:432–43.
41. Blohm U, Potthoff D, van der Kogel AJ, Pircher H. Solid tumors "melt" from the inside after successful CD8 T cell attack. *Eur J Immunol* 2006;36:468–77.
42. Thomas DA, Massagué J. TGF-beta directly targets cytotoxic T cell functions during tumor evasion of immune surveillance. *Cancer Cell* 2005;8:369–80.
43. Caramalho I, Faroudi M, Padovan E, Müller S, Valitutti S. Visualizing CTL/melanoma cell interactions: multiple hits must be delivered for tumor cell annihilation. *J Cell Mol Med* 2009;13:3834–46.
44. Schietinger A, Arina A, Liu RB, Wells S, Huang J, Engels B, et al. Longitudinal confocal microscopy imaging of solid tumor destruction following adoptive T cell transfer. *Oncoimmunology* 2013;2:e26677.
45. Benci JL, Xu B, Qiu Y, Wu TJ, Dada H, Twyman-Saint Victor C, et al. Tumor Interferon signaling regulates a multigenic resistance program to immune checkpoint blockade. *Cell* 2016;167:1540–54.e12.
46. Gong C, Milberg O, Wang B, Vicini P, Narwal R, Roskos L, et al. A computational multiscale agent-based model for simulating spatio-temporal tumor immune response to PD1 and PDL1 inhibition. *J R Soc Interface* 2017;14. Available from: <http://dx.doi.org/10.1098/rsif.2017.0320>.
47. Byrne HM. Dissecting cancer through mathematics: from the cell to the animal model. *Nat Rev Cancer* 2010;10:221–30.
48. Kather JN, Poleszczuk J, Suarez-Carmona M, Krisam J, Charoentong P, Valous NA, et al. In silico modeling of immunotherapy and stroma-targeting therapies in human colorectal cancer. *Cancer Res* 2017;77:6442–52.